Equilibrium Flows in Non-linear MHD Simulations of X-point Plasmas

S. PAMELA and G.T.A. HUYSMANS

Association Euratom-CEA, CEA/DSM/IRFM/SCCP/GTTM, Centre de Cadarache, 13108 Saint-Paul-Lez-Durance, France

Abstract. In non-linear MHD simulations of ELMs [1], a radially localised, toroidally symmetric, poloidal flow layer exists in the H-mode pedestal region. This sheared flow layer could have a significant influence on the linear stability properties of MHD instabilities and their non-linear evolution. Using the non-linear MHD simulation code JOREK [1] with reduced resistive MHD equations, we study the edge-localised poloidal flow in both circular and X-point tokamak plasmas at equilibrium (toroidal symmetry). For the circular case, an analytical interpretation is derived. In the simulations of X-point plasmas, the flow can have both $m = 0$ and $m = 1$ components. In fact, abrupt transitions take place between the two equilibrium states, accompanied by a strong increase in the kinetic energy. Similar transitions between equilibrium flow states have been predicted by Strauss [2] for m = 0 poloidal flow patterns. Scalings are obtained for both the $m = 1$ and $m = 0$ flows.

Keywords: ELMs, Equilibrium Poloidal Flow, JOREK, Transition
PACS: 52.30.-q, 52.55.Tn, 52.65.Kj

0. INTRODUCTION

In non-linear simulations of Edge-Localised-Modes with the 3D MHD code JOREK [1], a toroidally symmetric, poloidal flow is non-linearly induced by the instability (see Figure 1). This sheared flow layer is localised in the H-mode pedestal region and has a significant effect on the non-linear behaviour of ballooning instabilities. In particular, it separates density filaments away from the separatrix, and then reverses before cuting out another series of filaments, and so on until the end of the relaxation process.

Similar toroidally symmetric, poloidal flows also exist at the equilibrium (without toroidal harmonics, so without ballooning instabilities) [2],[3],[4]. They are driven by the H-mode pressure gradient, the diffusion and the asymmetry of the X-point geometry. A primary goal in applications of the JOREK code being the simulations of multiple ELM cycles, long simulations are involved; thus, the equilibrium is evolving constantly (even during non-linear phases), and it is important to understand the properties of such poloidal equilibrium flows and their evolution in long-time simulations. Here, we present results for circular plasmas in section 1 and introduce the study of flows with X-point geometry in section 2. In section 3, we detail transitions between different equilibrium flow patterns and end with the conclusion.

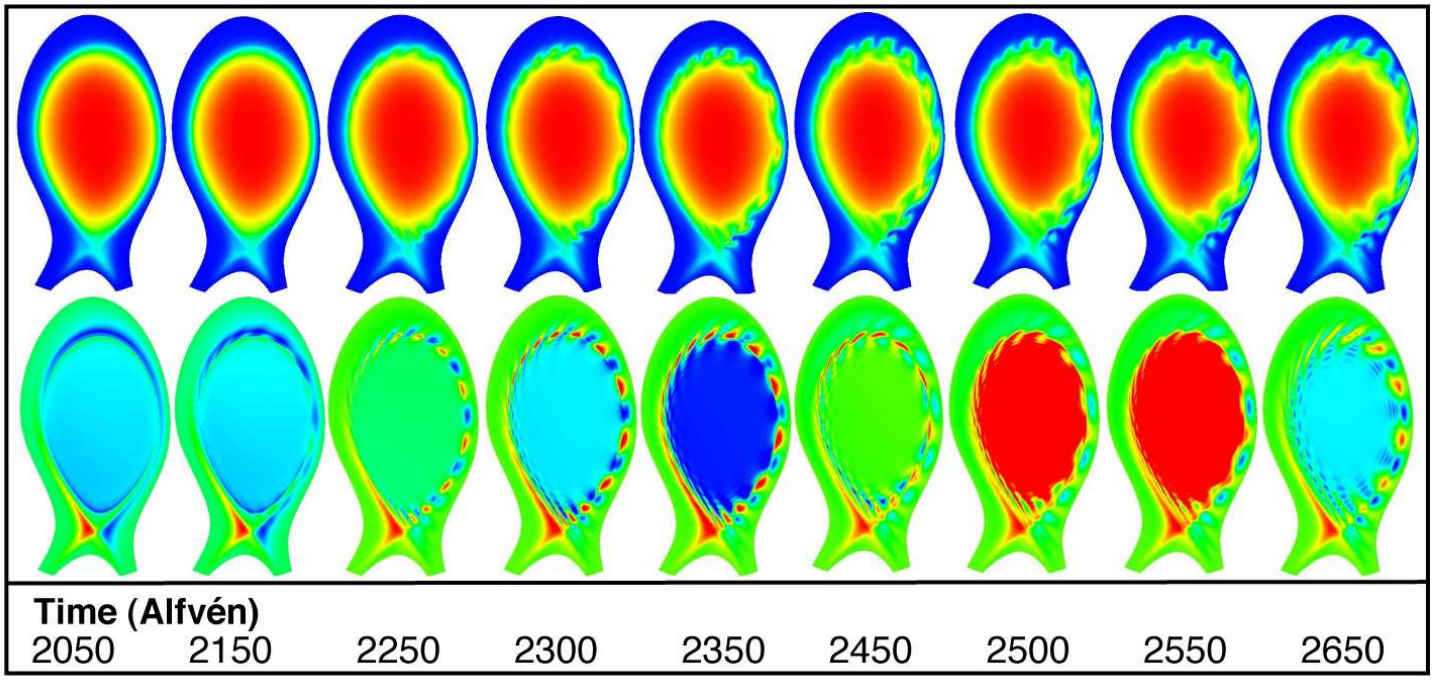

FIGURE 1. Non-linear Simulation of a Ballooning Mode (ELM). Top row shows the density filaments coming through the separatrix, and bottom row shows the electric potential with strong $m = 0$ structure.

1. POLOIDAL FLOW IN CIRCULAR PLASMAS

ELMs are known to occur only in H-mode plasmas, which means only in tokamaks with an X-point configuration; but before studying flows in such geometry, we shall start with circular plasmas. Here, the cause of the flow comes from the formation of a boundary layer near the wall. There are two convection cells, forming a m=1 $\sin\theta$ flow (θ is the poloidal angle). An analytical approach resulted in a scaling relating the thickness of the boundary layer to the viscosity μ and the resistivity η (the *Hartmann* number $\eta\mu$). The following equations are implemented in the JOREK code [1] (solved in weak form, but written here in strong form for analytical investigation)

$$\begin{aligned} R\left(\hat{\rho}\frac{\partial W}{\partial t}+\nabla\hat{\rho}\cdot\nabla_{\perp}\left(\frac{\partial u}{\partial t}\right)\right) &= \left[R^2\hat{\rho}W,u\right]-\frac{1}{2}\left[\hat{\rho},R^2\left|\nabla_{\perp}u\right|^2\right] \\ -\left[R^2,p\right]+\left[\psi,j\right]-\frac{1}{R}\frac{\partial j}{\partial\phi} &+ \mu\left(R\nabla^2\left(R^2W\right)-2\left[R^2,\frac{\partial u}{\partial Z}\right]\right) \qquad (1) \\ \rho\frac{\partial T}{\partial t} &= -\rho\boldsymbol{v}\cdot\nabla T-(\gamma-1)\rho T\nabla\cdot\boldsymbol{v} \\ &\quad +\kappa\nabla^2T+S_T \qquad (2) \\ \frac{\partial\psi}{\partial t} &= \eta\left(j-j_A\right)+R\left[\psi,u\right]-\frac{\partial u}{\partial\phi} \qquad (3) \end{aligned}$$

$$\frac{\partial \rho}{\partial t} = -\nabla \cdot (\rho \boldsymbol{v}) + D\nabla^2 \rho + S_\rho \tag{4}$$

where $R = R_0 + r\cos\theta$, $Z = r\sin\theta$, ϕ is the toroidal angle, $F_0 = R_0 B_0$, j_A is the applied current, u and ψ are the electric and magnetic potentials respectively, $W = \nabla \cdot \nabla_\perp u$ is the toroidal vorticity, $\hat{\rho} = \frac{R^2}{F_0}\rho$, $p = \rho T$ and $\boldsymbol{v} = \frac{R^2}{F_0}\nabla\phi \times \nabla u$ (no parallel velocity). S_ρ and S_T are the sources, and the Poisson Brackets are defined by $[a,b] = \boldsymbol{e}_\phi \cdot (\nabla a \times \nabla b)$.

For the circular geometry, the boundary conditions are that all variables u, ψ, W, j and T are taken to be zero at the wall. Because our interest concerns the equilibrium, and assuming the density to be fixed ($\rho = 1$), and the temperature profile to be known (ie. $\partial_r T = const = T_0'$), the two equations governing our equilibrium flow become

$$\begin{aligned} R_0[\psi, j] - \left[R^2, T\right] + \frac{\mu}{F_0} R\nabla^2\left(R^2 W\right) &= \\ \frac{1}{2F_0}\left[R^2, R^2|\nabla_\perp u|^2\right] - \frac{1}{F_0}\left[R^4 W, u\right] &+ 2\frac{\mu}{F_0}\left[R^2, \frac{\partial u}{\partial Z}\right] \end{aligned} \tag{5}$$

$$\eta(j - j_A) = \frac{R_0}{F_0} R[u, \psi] \tag{6}$$

Now, we represent the boundary layer by $r = a - \delta$ (a is the small radius, $\delta << 1$), and set $u = u_1 \sin\theta$ and $\psi = \psi_0 + \psi_1 \cos\theta$ with $\psi_1 << \psi_0$. All terms on right-hand side of equation (5) are negligible (higher δ-order) compared to the left-hand side. Developing the induction equation (6) and equating coefficients of $\cos\theta$ gives a result for u_1, thus leading to another set of equations

$$R_0[\psi, j] - \left[R^2, T\right] + \frac{\mu}{F_0} R\nabla^2\left(R^2 W\right) = 0 \tag{7}$$

$$\text{and} \quad u_1 = \frac{\eta a F_0 \psi_1}{\mu_0 R_0 \psi_0' \delta^2}. \tag{8}$$

where $\psi_0' = \frac{1}{\delta}\psi_0$. Now, the viscous term is very large inside the boundary layer (magnitude δ^{-6}) and negligible outside ($\mu \ll 1$). Also, assuming that $R_0[\psi, j] >> \left[R^2, T\right]$ inside the boundary layer would give $\psi_0' \sim \delta^{-2}$, contradicting continuity of ψ at the wall. Hence, we have that

$$\left[R^2, T\right] = R_0[\psi, j] \quad \text{outside the b.l.} \tag{9}$$

$$\left[R^2, T\right] = \frac{\mu}{F_0} R\nabla^2\left(R^2 W\right) \quad \text{inside the b.l.} \tag{10}$$

Note : this is because inside the boundary layer, there cannot be a static equilibrium between the two terms $\left[R^2, T\right]$ and $[\psi, j]$. Finally, substracting and using equation (8) gives the thickness of the boundary layer as a function of the Hartmann number

$$\delta = \sqrt{\frac{a}{\psi_0'}}\,(\mu\eta)^{\frac{1}{4}}. \tag{11}$$

Figure 2 shows a comparison of the analytical result (11) with the numerical simulations. Simulations show good agreement with the analytical approximation. Such numerical results have been achieved with simulations of X-point plasmas and will be presented. We first introduce the main properties of simulations and the principal characteristics of equilibrium flows in X-point geometry.

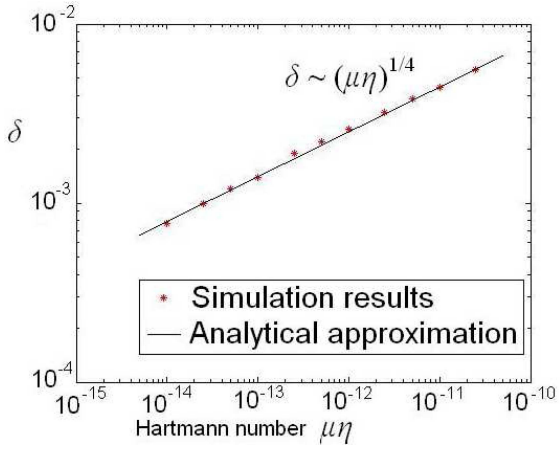

FIGURE 2. The thickness of the boundary layer from simulations is plotted as a function of the Hartmann number. The Analytical approximation fits with simulation results.

2. POLOIDAL FLOW IN X-POINT PLASMAS

In his paper, H.R. Strauss takes the origin of the flow to be the asymmetry of the plasma due to the X-point, together with the diffusion. The diffusion makes it possible for the temperature and density not to be aligned to the flux. In simulations with JOREK, this is the case for the density. According to Strauss, this perturbation is responsible for the flow.

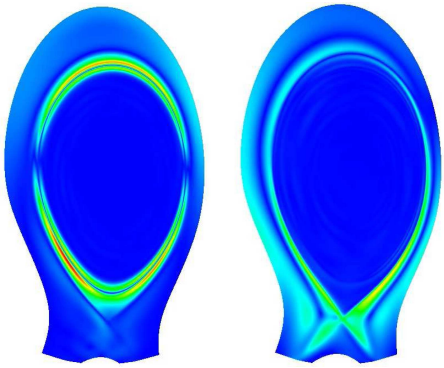

FIGURE 3. Flow Structures with Steep Pedestal (left) and Small Pedestal (right)

From equations (1-4), we may deduce the Pfirsch-Schlütter relation using $u = u_1 \sin(\theta)$, $j = j_A + j_1 \cos(\theta)$ and equation (6) to obtain $u_1 = -\eta j_1$, and considering only the biggest terms in (1), $[\psi, j] = [R^2, p]$, we get $-j_1 = \partial_r p$. Combinig

both results gives $u_1 = \eta \partial_r p$. Both dependencies (for η and for ∇p) are verified by the code. There is no relation between the flow amplitude and μ, but there is with $\kappa_\perp$ and $D_\perp$, as predicted by Strauss [2]. In fact, the smaller the conductivity, the stronger the influence, so that as $\kappa_\perp$ ranges down from 10^{-6} to 10^{-7}, the scaling goes from $v \sim \kappa_\perp^{0.25}$ to $v \sim \kappa_\perp^{0.5}$.

The relation between the width of the flow cells and the parameters η, μ, $\kappa_\perp$ or $D_\perp$ is not yet clear; in fact, it is the structure of the flow that is strongly affected by these parameters and, most of all, by the size of the pedestal. There are multiple flow structures and their presence depends on the parameters, but nevertheless, the most common structure (for steep pedestal gradients) is a sheared, $m = 1$ (sinusoidal) flow inside the separatrix (similar to the circular case). Figure 3 shows two extreme cases; combinations of these two patterns are observed as well. However, there are other stationary states, such as the $m = 0$ flow, and rapid transitions from one to the other are observed.

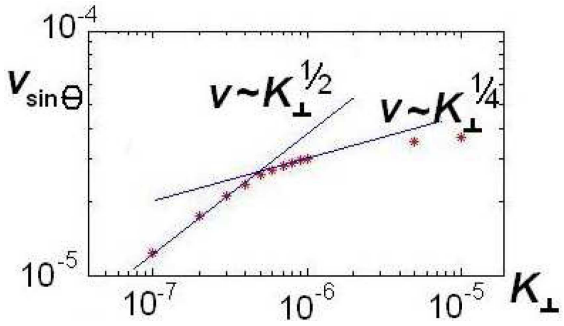

FIGURE 4. Scaling of the amplitude of the $m = 1$ component of the poloidal flow as a function of the perpendicular conductivity $\kappa_\perp$ (resistivity, viscosisity and diffusivity are constant at $\eta = \mu = D_\perp = 10^{-6}$).

3. TRANSITIONS BETWEEN EQUILIBRIUM FLOW STATES

It is important to understand the linear background of a non-linear simulation. In the case of ballooning instabilities (ELMs), long simulations are involved (from 1000 up to 10000 Alfvén times per relaxation, so up to $\sim 10ms$). Furthermore, one of the main goals of the study of ELMs with the JOREK code is the achievement of multiple ELMs simulations (which would imply simulations of about 10^5 Alfvén times and more). Therefore, the evolution of the equilibrium has to be investigated in order to understand its influence, if any, on the non-linear behaviour of ballooning instabilities. Of course, if the density source and heating are adjusted according to the diffusivities, the density and temperature profiles will remain unchanged, and so will the flow. However, an ELM relaxation involves drastic changes in density and temperature profiles, and as observed in long simulations of equilibrium, such falls of the gradients strongly affect the equilibrium flow.

There are different stationary flow states, and abrupt transitions may occur from one state to the other (see Figure 5). Such sharp transitions between multiple flow states had been predicted by Strauss [2]. In JOREK simulations, we observe transitions from an $m = 1$ $\sin\theta$ flow to an $m = 0$ flow. This rapid change takes place after around 10^4 to

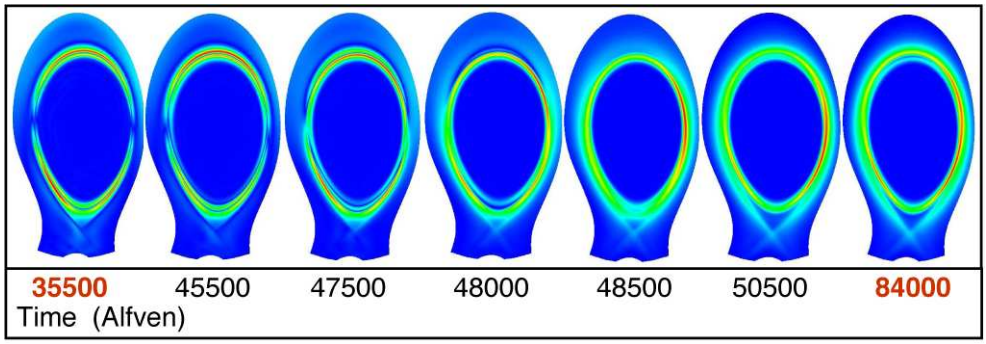

FIGURE 5. Transition between a predominantly $m = 1$ flow to an $m = 0$ flow structure with an increase in the kinetic energy

10^5 Alfvén times (depending on the parameters), and only if the pedestal gradient is declining. In fact, the density and the flow are tightly related, and the transition comes with an inward shift of the density. This might come from the fact that equations (1) to (4) solved in JOREK don't include the parallel velocity (neglected). With $v_{\|}$, the density might stay aligned with the flux ψ. In fact, it has to be verified that this transition occurs when the code solves the equations with $v_{\|}$. However, despite the decay of the gradients, the kinetic energy suddenly steps up at the transition (ie. the flow amplitude jumps increases, see Figure 6).

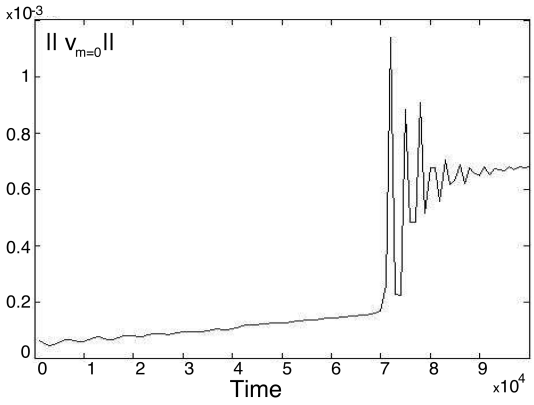

FIGURE 6. The $m = 0$ flow amplitude as a function of time showing a sharp transition.

Using the Fourier method to extract the $m = 0$ and $m = 1$ components of the flow, we can scale the $m = 0$ flow with the different parameters. Again, the strongest relation is with the resistivity, but the scaling changes with the transition, so that $v_{m=0} \sim \eta$ before the transition, and $v_{m=0} \sim \eta^{1/2}$ afterwards. There is also a relation to the diffusivities very similar to the one seen in Figure 4. More scalings need to be done, but as predicted by Strauss, the diffusion does play a role in the origin of the flow and the transitions.

4. CONCLUSION

For flows in a circular plasma bounded by a wall, we derived an analytical relation between the thickness of the flow boundary layer and the Hartmann number. For X-point plasmas, as in Strauss' paper, diffusion is connected to the origin of the equilibrium flow, eventhough the different patterns of this flow are mostly related to the resistivity. A sharp transition takes place between the $m = 1$ and the $m = 0$ patterns, and comes together with a jump in kinetic energy. This transition will be further investigated. The next step is the study of the influence of the equilibrium flow on the non-linear stability of ballooning modes.

REFERENCES

[1] G.T.A. Huysmans and O. Czarny, MHD stability in X-point geometry: simulation of ELMs, *Nucl. Fusion* **47** No 7 (July 2007) 659-666.

[2] H.R. Strauss, *Phys. Plasmas* **2**, 1229 (1995).

[3] A.Y. Aydemir, Shear flows at the tokamak edge and their interaction with edge-localized modes, *Phys. Plasmas* **14**, 056118 (2007).

[4] H.P. Zehrfeld, Dissipative Magnetohydrodynamic Equilibria with Compressible Fluid Flow, *European Phys. Society* (2000)